Available online at www.sciencedirect.com
SCIENCE DIRECT®
Thermochimica Acta 419 (2004) 19–29
thermochimica acta
www.elsevier.com/locate/tca

Quantification of low levels of amorphous content in maltitol

M. Hurtta*, I. Pitkänen

Department of Chemistry, University of Jyväskylä, P.O. Box 35, Fin-40014 Jyväskylän Yliopisto, Finland

Received 1 July 2003; received in revised form 8 January 2004; accepted 8 January 2004

Available online 11 March 2004

Abstract

A method for the quantification of low levels of amorphous content of maltitol with hyper-DSC (high speed DSC) was developed. The method is based on the fact that the change of specific heat (ΔC_p) at the glass transition is linearly proportional to the amorphous content. Twelve synthetic mixtures with various degrees of crystalline and amorphous maltitol were prepared. ΔC_p was determined at both fictive and half point glass transition temperature and equations for ΔC_p as a function of amorphicity were calculated. The limit of detection (LOD) and the limit of quantification (LOQ) values were 0.313% (amorphicity) and 1.04% for fictive temperature and 0.107 and 0.358% for half point temperature, respectively. In addition, instrumental sensitivity and detection limit were determined. The calculated LOD value for a heating rate of 100 °C min^{-1} and a 10 mg sample was 0.001%. It was noticed that the preparation of amorphous maltitol was the weakest point in the quantification of low amorphous levels in maltitol. The influence of annealing time and the heating/cooling rate on the ΔC_p was studied. The influence of moisture was discussed.

Keywords: Maltitol; Thermal analysis; Amorphicity; Glass transition; Hyper-DSC

1. Introduction

Quantification of residual amorphous content is an important and difficult problem and many techniques have been used to solve it [1,2]. X-ray powder diffraction is a method used to study crystallinity and polymorphism. The determination of amorphous content with X-rays is based on background absorption. As the absorption signal is small compared with the intensity of peaks in a crystalline sample, this method is not very sensitive for that purpose. Thermal methods have also been used for amorphous content determination. In differential scanning calorimetry (DSC), the determination is traditionally based on the determination of melting entalphy. When the melting entalphy of a 100% crystalline sample is known, amorphicity is determined as the difference between a 100% crystalline sample and the test sample. In this technique a minor amorphous content causes a small change in the total signal, and consequently it is difficult to detect with confidence [2]. In DSC, amorphous content can also be determined directly from the change of specific heat capacity (ΔC_p) at glass transition region.

There is a wide variety of different DSC techniques. Conventional DSC is based on a linear heating rate. In temperature modulated DSC (TMDSC) a small sinusoidal temperature modulation is applied to the sample in addition to the usual linear ramp. In the newest technique, hyper-DSC, controlled fast heating and cooling rates of 50 °C min^{-1} up to 500 °C min^{-1} are used [3]. This significantly increases the sensitivity because the increased scan rate leads to higher heat flow. Whereas amorphous character can be difficult to detect in highly crystalline solids using conventional DSC technique, hyper-DSC can show glass transitions with much increased sensitivity and less time [3].

Amorphous materials may exist as solid glasses or liquid-like rubbers. The transition between these states is a second-order change in phase, which occurs at the glass transition temperature, T_g [4]. There are at least three ways to determine T_g. Standard T_g is the temperature corresponding to the point on the heat flow curve where the specific heat change is 50% of the change in the complete transition. This is the temperature at which the heat capacity is midway between the liquid and glassy states [5]. The glass transition can also be taken as the inflection point of the DSC curve associated with the glass transition. If a high relaxation peak follows the glass transition, the inflection

* Corresponding author. Fax: +358-142602501.
E-mail address: mihurtta@cc.jyu.fi (M. Hurtta).

0040-6031/$ – see front matter © 2004 Elsevier B.V. All rights reserved.
doi:10.1016/j.tca.2004.01.024

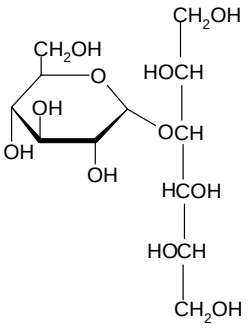

Fig. 1. Molecular structure of maltitol.

point of the DSC curve can change from the real inflection point of the glass transition. The fictive temperature refers to the point on the enthalpy curve where the change of slope occurs [6]. The enthalpy curve is the integral of the specific heat curve. The fictive temperature is the intersection of the extrapolated pre-transition and post-transition baselines on the enthalpy curve.

The ΔC_p is linearly proportional to the amorphous content in case that the amorphous glasses are in the same state. The largest change in the specific heat is equal to the difference of crystalline and rubber states. When the glass transition is used for the quantification of the amorphous content, there has to be a reference material. A starting point for the development of this method is to ensure that the change of the specific heat of a 100% amorphous sample is reproducible. Many things influence ΔC_p. Glasses are known to change their properties when annealed at below their glass transition temperature. The release of the relaxation enthalpy that follows the glass transition corresponds to the enthalpy difference between the annealed and the quenched (non-annealed) glass [7]. Different cooling rates produce glasses of different degree of order. The structure of non-annealed glass is close to the structure of liquid state and the change of specific heat is smaller for non-annealed than annealed glass [5]. In addition, the glass transition temperatures of amorphous sugars and sugar alcohols are extremely sensitive to water. The differences between reported T_g values for the same sugar of sugar alcohol are probably due to residual water in samples, differences in sample handling techniques, and differences in techniques used to measure T_g [8,9].

The aim of this study was to find out if it is possible to develop a method for the quantification of the low levels of amorphous content of sugars and sugar alcohols. The method was based on the specific heat change in the glass transition region measured by hyper-DSC. The test sample chosen was maltitol (4-*O*-A-D-glucopyranosyl-D-glucitol: $C_{12}H_{22}O_{11}$). The molecular structure of maltitol is shown in Fig. 1. The crystal structure of maltitol has been determined by X-ray diffraction [10–12]. Some thermodynamic data for maltitol were found in the literature (the melting temperature and the heat of fusion) [4,7,12–15]. The glass transition temperature and the change in specific heat capacity have also been determined [4,7,13,14]. In experimental work maltitol has occurred only in one form (no polymorphism was observed). In addition, no trace of recrystallization was detected in the glass transition range during the measurements [7]. Once melted, maltitol can be undercooled without further cold crystallization [14].

Maltitol and its glass transition have been discussed in the literature and different techniques have been used in its study. Lebrun and Miltenburg [13] used an adiabatic calorimeter to measure the heat capacity of maltitol in all condensed states (liquid, metastable liquid, solid and glass). They also determined the change of the heat capacity at T_g and the temperature dependence of the configurational entropy [13]. Bustin and Descamps [14] used MDSC to study the glass transition of maltitol. Claudy et al. [7] used conventional DSC to study the influence of the annealing on the glass transition temperature of maltitol glass. Also we discuss maltitol and its glass transition in this study but our approach is different. In this work we studied some of the factors that influence the magnitude of the specific heat change at the glass transition region. All the articles quoted report only the values of T_g and ΔC_p, but our study demonstrated that the temperature at which the ΔC_p is calculated influences the results. On the basis of these observations we developed a method of quantification of low levels of amorphous content in maltitol.

2. Experimental

Crystalline maltitol (Lot M010803) was obtained from Danisco Sweeteners and its purity was 99.8% (determined by HPLC by Danisco Sweeteners).

Amorphous maltitol was prepared from crystalline maltitol by melting it in an oven at 165 °C (mp 150 °C) and keeping it at that temperature for 15 min. The degradation temperature of maltitol was checked with TG before the preparation of amorphous maltitol. The bright and colourless liquid was poured on to a cooled metal plate and the plate was put in a desiccator. The desiccator was refrigerated at 5 °C at least for 1 h. The final product (glass) was glassy "pearls." After cooling, amorphous maltitol was crushed in a porcelain mortar. Amorphous maltitol powder was stored in a desiccator over P_2O_5 at 5 °C. Experiments showed that the powder started to crystallize if it was stored outside the desiccator at room temperature; the change started in a couple of hours. The moisture content of crystalline maltitol was measured with TG but that of amorphous maltitol was not measured.

The DSC measurements were carried out on a Perkin-Elmer DSC Diamond using 50 μl aluminium sample cups with capillary holes. The temperature calibration was carried out by deionized water, indium (Indium Reference Material, PE P/N 0319-0033) and zinc (Zinc Reference Material, PE P/N 0319-0036), and the heat flow was calibrated by the melting enthalpy of indium or by the specific heat of sap-

phire (Sapphire Disc Standard, 0219-0136 REV C, Heat Kit, QTY 1 10-25-95). The specific heat method used the specific heat of sapphire over a user-defined temperature range. The baseline and sample curves were measured and the calibration was then built automatically. The calibration was checked before running samples by measuring the melting enthalpy of indium at same heating rate as the proper measurements were done. All measured glass transition temperatures were corrected for thermal lag (0.056 min). Indium was measured by different heating rates. The onset values as function of heating rate were drawn and the linear regression was calculated. The thermal lag was the slope of the regression curve. In final values, the heating rate was noticed before correction was done.

For the determination of the effect of the heating or cooling rate on the glass transition temperature and the change of the specific heat capacity a different test series was performed. Measurements were obtained in a series of cooling and heating cycles without removing the sample from DSC. The sample weight was about 5 mg. Amorphous maltitol was produced in DSC by heating crystalline compound above the melting point to 165 °C before the measurements. The temperature range was 0–100 °C. Heating and cooling rates were changed. The influence of annealing on ΔC_p was investigated. The annealing temperature was 40 °C [14]. The annealing times 35 and 60 min were tested. In addition, the heat flow and specific heat calibration methods were tested. The time temperature sequence of the experiments is shown in Fig. 2 and the parameters of different series are shown in Table 1.

The specific heat curves were determined for crystalline maltitol, quenched (non-annealed) glass, and annealed glass. The measurements were done using a classical three-curve C_p method. The temperature range was 0–165 °C and the heating rate was 10 °C min^{-1}. The annealing temperature was 40 °C and the time 60 min for annealed glass. The equations for crystalline, liquid amorphous and annealed amorphous materials were calculated from the specific heat curves.

Synthetic mixtures were prepared by weighing known quantities of amorphous and crystalline maltitol at various ratios (0.1, 0.5, 1, 5, 7.5, 10, 15, 20, 25, 50, 75 (w/w) amorphous content) and by mixing them thoroughly in a porcelain mortar. In addition, approaching 100 and 0% amorphous samples were used. Crystalline samples were dried and stored over P_2O_5 before and between preparing synthetic mixtures. The amorphous powder was also stored in a P_2O_5 desiccator at 5 °C; however, a remarkable problem was noted in preparing synthetic mixtures. The desiccator was moved from a refrigerator (5 °C) to the room temperature (22 °C) at the beginning of the work. The amorphicity was checked by DSC (no melting peaks were noticed) before the preparation of mixtures was started. As the synthetic mixtures were not stable, the mixtures were done one at the time and measured immediately. Two to five parallel measurements were taken at each test point. The sample weights were 8–10 mg. The temperature range was −10 to 100 °C. The annealing time was 60 min and the temperature 40 °C. The following temperature program was used to run the experiments:

(1) hold for 1 min at 30 °C,
(2) heat from 30 to 40 °C at 10 °C min^{-1},
(3) hold for 60 min at 40 °C,
(4) cool from 40 to −10 °C at 10 °C min^{-1},
(5) hold for 1 min at −10 °C,
(6) heat from −10 to 100 °C at 100 °C min^{-1},
(7) hold for 1 min at 100 °C.

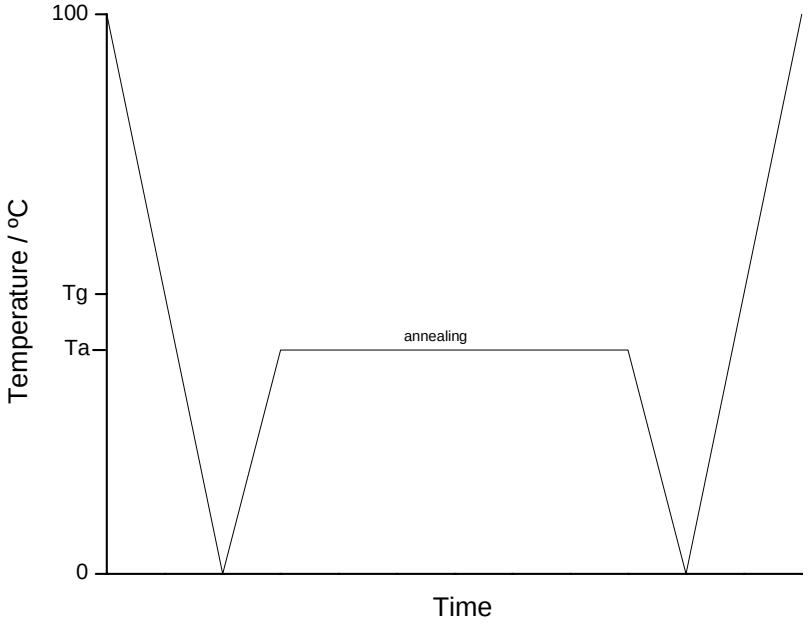

Fig. 2. The time–temperature sequence of ΔC_p measurements.

Table 1
The measuring methods for the determination of ΔC_p

Series	Cooling rate (°C min^{-1})	Heating rate (°C min^{-1})	Annealing time (min)	Calibration method[a]
1	1, 5, 10, 50, 100	10	0	1
2	1, 5, 10, 50, 100	100	0	1
3	10	1, 5, 10, 50, 100	0	1
4	100	1, 5, 10, 50, 100	0	1
5a	2, 5, 10, 25, 50, 70, 100, 200	10	0	1
5b	2, 5, 10, 25, 50, 70, 100, 200	10	35	1
6	2, 5, 10, 25, 50, 70, 100, 200	10	60	1
7	2, 5, 10, 25, 50, 70, 100, 200	10	60	2

[a] Heat flow calibration done by (1) the melting enthalpy of indium and calibration heating rate 2 °C min^{-1}; (2) the specific heat of sapphire and calibration heating rate 10 °C min^{-1}.

3. Results and discussion

3.1. The change of the specific heat at glass transition

The fictive temperature, half point temperature, the specific heat change and the relaxation enthalpy were calculated (Fig. 3). The results of T_g and ΔC_p studies are in Tables 2 and 3. It is possible to draw the following conclusions from these tables. The fictive glass transition temperature is lower than the corresponding half point temperature. Increasing the heating rate changes both values to higher temperatures nearly in the same way in the quenched glass [7]. This observation is in conflict with the literature concerning fictive temperature, which in all cases describes the fictive temperature as being independent of heating rate and only dependent on cooling rate [16,17]. Here the reason for this anomalous fictive temperature behaviour is different amount of annealing under the glass transition. When heating rate is increased, onset and end temperatures of the glass transition move to higher temperatures due to the thermal resistance. The change of cooling rate does not influence the half point temperature. The effect of heating rate on the heat flow data is illustrated in Fig. 4.

On the basis of Table 2, the fictive temperature should increase when cooling rate increases. However, the fictive temperature does not change in series 5b, 6 and 7 in Table 3 although cooling rate changes. In fact, the fictive temperature depends on the relaxation enthalpy instead of the cooling rate. A high relaxation enthalpy lowers the fictive temperature. The changes of specific heat values are nearly equal for both fictive and half point temperatures.

Annealing causes the ΔC_p at T_g to become more stable but there is still some dispersion between the different measurements at different cooling rates (series 5). At longer annealing time (series 6), ΔC_p at T_g becomes more and more constant between different measurements. The onset temperature of the half point glass transition moves to higher temperature as annealing time increases. The enthalpy of the relaxation peak changes as well.

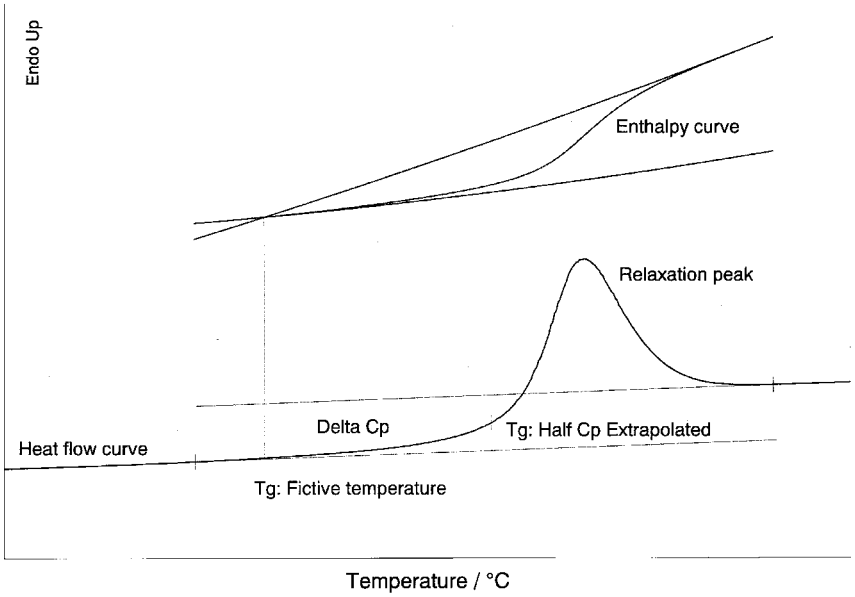

Fig. 3. Calculated parameters. Fictive temperature reports the point on enthalpy curve where the change of slope occurs. Half C_p extrapolated reports the point on heat flow curve where the specific heat change is half on the change in the complete transition. Relaxation enthalpy was calculated from the area of the relaxation peak.

Table 2
The effect of heating/cooling rate on ΔC_p. Measuring methods are in Table 1

Series	Cooling/heating rate (°C min^{-1})[a]	Fictive temperature		Half point temperature		Relaxation		
		T_g (°C)	ΔC_p (J g^{-1} K^{-1})	T_g (°C)	ΔC_p (J g^{-1} K^{-1})	Onset (°C)	Peak (°C)	ΔH (J g^{-1})
1	1	43.08	0.52	48.51	0.56	50.38	52.69	2.54
	5	45.32	0.51	48.19	0.53	50.18	52.19	1.17
	10	46.15	0.50	48.38	0.50	50.18	52.20	0.89
	50	46.65	0.44	48.55	0.46	50.36	52.37	0.67
	100	47.44	0.52	48.83	0.51	50.69	52.37	0.50
2	1	47.78	0.70	56.31	0.66	58.11	61.03	4.91
	5	49.68	0.66	54.91	0.62	56.83	59.77	2.66
	10	50.47	0.61	54.70	0.58	56.59	59.45	1.98
	50	51.61	0.61	54.12	0.61	56.77	59.38	0.88
	100	52.64	0.45	54.90	0.43	56.84	59.28	0.84
3	1	47.08	0.65	47.02	0.67			
	5	45.27	0.50	47.07	0.49	48.81	50.82	0.66
	10	45.78	0.58	47.99	0.57	49.88	52.00	0.84
	50	48.05	0.60	51.94	0.57	53.87	56.40	1.68
	100	50.28	0.65	54.76	0.64	56.91	59.77	2.04
4	1	46.18	1.11	46.10	1.08			
	5	45.69	0.59	46.83	0.61	49.13	50.89	0.49
	10	46.69	0.63	48.07	0.63	50.53	52.21	0.44
	50	50.18	0.57	52.09	0.55	54.89	56.58	0.67
	100	53.84	0.52	55.59	0.48	58.63	60.31	0.57

[a] Cooling rate in series 1 and 2, heating rate in series 3 and 4.

In the series 1–6 the calibration was done at a heating rate of 2 °C min^{-1} and the heat flow calibration was carried out with the melting enthalpy change of indium. The apparatus was calibrated again, now at a heating rate of 10 °C min^{-1}, and the heat flow was calibrated with the specific heat of sapphire. It was noticed that it was better to do a calibration at the same parameter as was used in measurements. The heat flow calibration carried out with the specific heat of sapphire gave a better baseline for the hyper-DSC technique. After a new calibration (series 7) it was noticed that eight different cooling rates gave almost the same results. The outcome was a measuring program, which produced a constant ΔC_p at

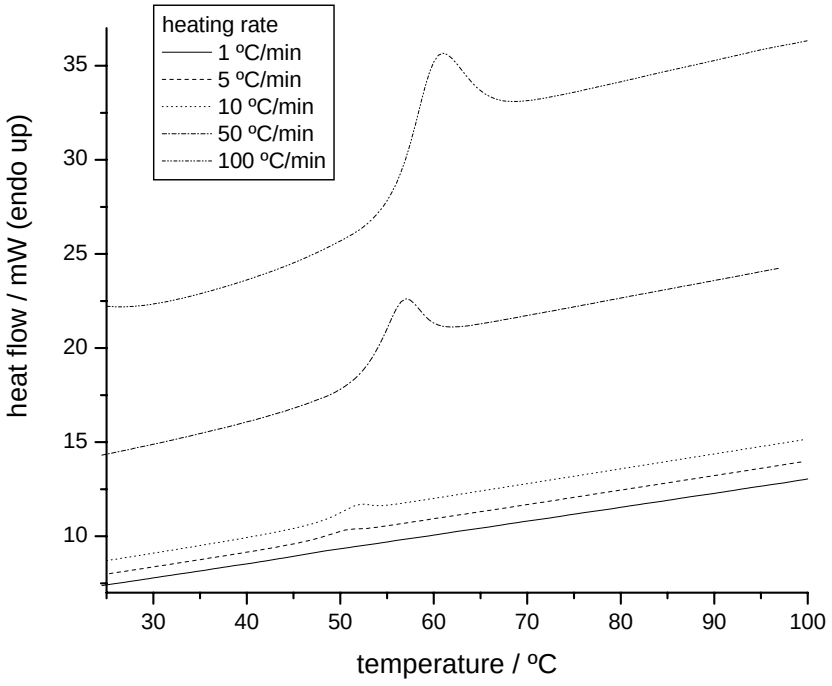

Fig. 4. The effect of heating rate on the heat flow data. Raw data is from series 3 (no baseline correction).

Table 3
The effect of annealing time and calibration method on ΔC_p (measuring methods are in Table 1)

Annealing time (min)	Cooling rate (°C min^{-1})	Fictive temperature		Half point temperature		Relaxation		
		T_g (°C)	ΔC_p (J g^{-1} K^{-1})	T_g (°C)	ΔC_p (J g^{-1} K^{-1})	Onset (°C)	Peak (°C)	ΔH (J g^{-1})
0 (series 5a)	2	42.92	0.52	47.64	0.54	49.81	52.39	1.92
	5	44.80	0.54	47.98	0.53	49.90	52.23	1.22
	10	44.97	0.52	47.86	0.52	49.88	52.15	1.02
	25	46.15	0.51	48.35	0.50	50.29	52.22	0.72
	50	46.81	0.58	48.51	0.57	50.63	52.39	0.50
	75	46.61	0.53	48.49	0.53	50.55	52.31	0.55
	100	46.62	0.58	48.35	0.59	50.63	52.40	0.52
	200	46.36	0.54	48.33	0.54	50.47	52.40	0.59
Mean		45.65	0.54	48.19	0.54	50.27	52.31	0.88
S.D.		1.34	0.03	0.32	0.03	0.35	0.10	0.49
35 (series 5b)	2	42.31	0.59	48.85	0.64	50.97	53.22	3.43
	5	41.23	0.50	48.53	0.56	50.68	53.05	3.42
	10	41.12	0.51	48.49	0.54	50.62	53.05	3.39
	25	42.06	0.56	48.59	0.58	50.66	53.04	3.13
	50	41.97	0.56	48.60	0.58	50.56	52.88	3.23
	75	41.36	0.52	48.39	0.56	50.53	52.89	3.29
	100	42.47	0.60	48.56	0.61	50.61	52.89	3.10
	200	42.56	0.60	48.59	0.62	50.64	52.89	3.04
Mean		41.88	0.56	48.57	0.58	50.66	52.99	3.25
S.D.		0.57	0.04	0.13	0.03	0.14	0.12	0.15
60 (series 6)[a]	2	41.91	0.59	49.17	0.57	51.32	53.56	3.72
	5	41.52	0.56	48.92	0.56	51.22	53.40	3.65
	10	41.51	0.56	48.83	0.60	51.15	53.39	3.66
	25	41.13	0.54	48.59	0.60	51.08	53.40	3.56
	50	40.77	0.51	48.61	0.58	51.06	53.40	3.53
	75	41.91	0.59	48.71	0.63	51.09	53.40	3.46
	100	41.88	0.57	48.85	0.59	51.08	53.40	3.45
	200	41.80	0.56	48.90	0.58	51.08	53.40	3.47
Mean		41.55	0.56	48.82	0.59	51.13	53.42	3.56
S.D.		0.42	0.03	0.19	0.02	0.09	0.06	0.10
60 (series 7)[a]	2	41.65	0.60	49.03	0.56	51.16	53.23	3.76
	5	42.02	0.61	48.88	0.57	51.19	53.05	3.64
	10	41.70	0.61	48.87	0.59	51.15	53.05	3.61
	25	41.93	0.60	49.09	0.56	51.13	53.05	3.72
	50	42.11	0.61	49.09	0.57	51.18	53.06	3.61
	75	41.98	0.61	49.03	0.58	51.33	53.06	3.63
	100	41.96	0.61	49.06	0.57	51.33	53.06	3.65
	200	42.00	0.61	49.09	0.57	51.28	53.06	3.63
Mean		41.91	0.61	49.01	0.57	51.21	53.08	3.66
S.D.		0.17	0.01	0.09	0.01	0.09	0.07	0.06

[a] Heat flow calibration done by the melting enthalpy of indium in series 6 and by the specific heat of sapphire in series 7.

T_g. Therefore it was concluded that the method was suitable for the measurements of synthetic mixtures of amorphous and crystalline maltitol. Faster heating rates were used for synthetic mixtures because of the increased sensitivity.

Six parallel measurements were made for 100% amorphous maltitol to study the precision of the measurements. Preparation of amorphous samples was done in DSC by heating above the melting point (150 °C) and thereafter cooling them to the glass phase in the same way for all samples. Crystalline maltitol was dried over P_2O_5 before measurements. The results are in Table 4. The mean of ΔC_p for six parallel measurements was 0.727 ± 0.029 J g^{-1} K^{-1} for the fictive and 0.706 ± 0.035 J g^{-1} K^{-1} for the half point temperature. The values of ΔC_p are higher than in series 7 (Table 3). The main reason is probably moisture because the crystalline maltitol used was now dried just before measurement and in series 7 it was done earlier. The moisture reduces ΔC_p. The results of series 7 refer to maltitol preserved in the usual temperature and moisture of room and those in Table 4 refer to dried samples under carefully controlled conditions.

The reported values of thermodynamic data of maltitol are given in Table 5. In the values given for this work, dried sample means that crystalline maltitol had been dried over

Table 4
The results of parallel measurements of 100% amorphous sample

	Sample weight (mg)	Fictive temperature		Half point temperature		Relaxation		
		T_g (°C)	ΔC_p (J g^{-1} K^{-1})	T_g (°C)	ΔC_p (J g^{-1} K^{-1})	Onset (°C)	Peak (°C)	ΔH (J g^{-1})
1	4.648	41.85	0.75	52.64	0.73	54.53	57.89	6.49
2	4.896	42.52	0.73	52.96	0.70	56.19	57.87	5.81
3	5.190	42.15	0.67	52.95	0.64	54.49	57.84	6.34
4	5.066	42.22	0.74	52.84	0.72	56.15	57.84	5.72
5	5.314	42.19	0.75	52.91	0.74	56.18	57.56	6.20
6	5.410	42.63	0.73	53.01	0.69	56.15	57.83	5.96
Mean		42.26	0.73	52.89	0.71	55.61	57.80	6.09
S.D.		0.28	0.03	0.13	0.04	0.86	0.12	0.31

Amorphous maltitol was produced in DSC by heating the crystalline compound above its melting point before measurements. Crystalline maltitol was dried over P_2O_5 before measurements.

P_2O_5 just before measurements and non-dried sample means that there was no additional drying before measurements. Although the values of T_g and ΔC_p vary a little between different references, they are comparable with our results. All these values refer to annealed samples. Lebrun Miltenburg [13] and Claudy et al. [7] obtained values of ΔC_p that are equal to our results for dried samples determined by the half point method. On the other hand, the values of Roos [8] and Bustin and Descamps [14] are close to our values for non-dried samples.

3.2. Specific heat measurements

The experimental specific heat curves for crystalline, non-annealed (quenched), and annealed amorphous samples are shown in Fig. 5. Specific heat is due mainly to on intramolecular and intermolecular vibrations in solid glass and crystalline state. There is also translation movement in rubber and liquid state. Therefore these specific heats are higher than the specific heats of solid state. On the other hand, the specific heat of quenched glass is higher than the specific heat of annealed glass, and analogously, the specific heat of annealed glass is higher than the specific heat of crystal. According to Claudy et al. [7] maltitol molecules are associated in the liquid state:

$$\mathrm{mM} \leftrightarrow \mathrm{M_m}$$

These associations involve hydrogen or van der Waals bonding. These molecular associations can further associate in annealing:

$$\mathrm{M_m} + \mathrm{M_m} \leftrightarrow (\mathrm{M_m})_2, \ldots, (\mathrm{M_m})_{n-1} + \mathrm{M_m} \leftrightarrow (\mathrm{M_m})_n$$

The structure of the quenched glass is same as the rubber state. The annealed glass is more organised especially over short distances but it lacks the long-distance order of the crystal structure.

The specific heat curves for crystalline, annealed amorphous glass and amorphous rubber samples were calculated [13]. The software used was Microcal Origin [18]. The result is given in the following three equations and correlation coefficients:

$$C_p\,(\text{crystalline}) = 1.138 + 0.00461t\,(^\circ\mathrm{C}), \quad R = 0.9996$$

Table 5
Literature values of glass transition temperature (T_g), the change of specific heat (ΔC_p), melting peak (T_m) and the heat of fusion (ΔH)

Method	T_g (°C)	ΔC_p (J g^{-1} K^{-1})	T_m (°C)	ΔH (J g^{-1})	Reference
Hyper-DSC					
Dried sample			150.3[a]	164.4	This work
Fictive	42.3	0.73			This work
Half point	52.9	0.71			This work
Non-dried sample			150.6[a]	162.2	This work
Fictive	41.9	0.61			This work
Half point	49.0	0.57			This work
Adiabatic calorimeter	38	0.707	147	159.9	Lebrun and Miltenburg [13]
Modulated DSC	49	0.610	147	156.8	Bustin Descamps [14]
DSC	50	0.72	145	–	Claudy et al. [7]
DSC	44	0.56	149	147	Roos [4]
DSC	–	–	147	164	Ohno and Hirao [12]

Literature values given in J mol^{-1} K^{-1} have been converted to J g^{-1} K^{-1} in this table.
[a] Heating rate 2 °C min^{-1}, peak temperature.

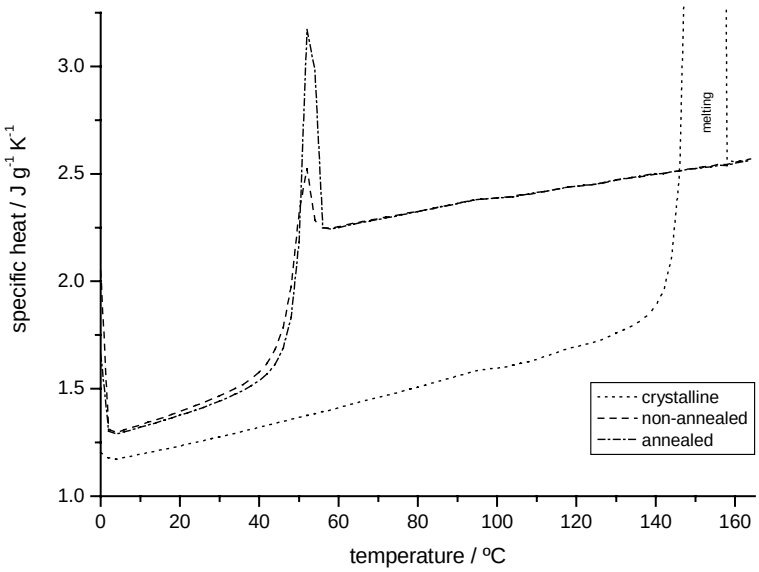

Fig. 5. The experimental specific heat curves for crystalline, non-annealed amorphous and annealed amorphous maltitol.

C_p (annealed amorphous glass)

$$= 1.264 + 0.00566t\ (^\circ\mathrm{C}), \quad R = 0.9994$$

C_p (amorphous rubber)

$$= 2.070 + 0.00315t\ (^\circ\mathrm{C}), \quad R = 0.9953$$

The dependence of the specific heat on temperature is obtained by calculating C_p at different temperatures near the glass transition temperature. As can be seen in Table 6, the temperature influences the values. There is a difference between the values but the variation is not very large. The hypothetical maximum change in ΔC_p is the difference between the crystalline and amorphous rubber states. In addition, a difference between amorphous rubber and annealed amorphous glass has been calculated. These calculated values correspond to the values of measured 100% annealed amorphous sample.

3.3. Synthetic mixtures

Difficulty was experienced with the synthetic mixtures of crystalline and glass maltitol because the composition of mixtures changed in storage. Three to six parallel points were measured of every lot, but it was noticed that some of the results were incorrect as a result of too long storage time. That became evident by examining how long the mixture was stored before the measurements. A significant effect was also caused by the length of the time the amorphous maltitol was stored before the mixture was prepared. The results of the changed mixtures were rejected and the remaining points were used to calculate average and standard deviation values for every lot. For comparison, the glass transition temperature and the specific heat change were calculated for both fictive and half point temperatures. The change of the specific heat at the glass transition temperature as a function of the amorphicity and the linear regression lines with R (correlation coefficient) values are illustrated in Fig. 6. The equations are:

Fictive temperature :

$$\Delta C_p = 0.00214 + 0.00702\times, \quad R = 0.997$$

Half point temperature :

$$\Delta C_p = 0.00153 + 0.00682\times, \quad R = 0.996$$

Table 6
The effect of temperature on the calculated specific heat and the theoretical change of specific heat at glass transition region

Temperature (°C)	Calculated specific heat (J g^{-1} K^{-1})			Difference (J g^{-1} K^{-1})[a]	
	Crystalline	Annealed amorphous glass	Amorphous rubber	1	2
30	1.277	1.434	2.164	0.888	0.730
35	1.300	1.463	2.180	0.881	0.718
40	1.323	1.491	2.196	0.873	0.705
45	1.346	1.519	2.212	0.866	0.692
50	1.369	1.547	2.227	0.859	0.680
55	1.392	1.576	2.243	0.851	0.667

[a] Difference 1 = the theoretical change of specific heat of rubber and crystalline; difference 2 = the theoretical change of specific heat of rubber and annealed amorphous glass.

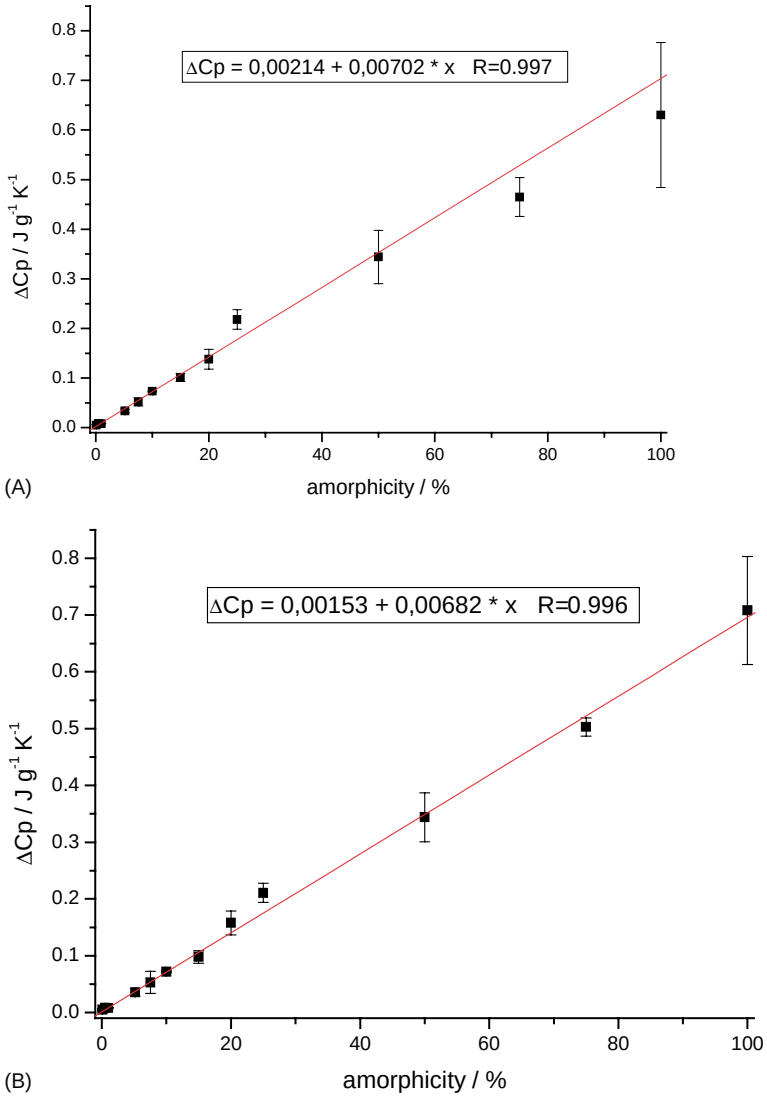

Fig. 6. Average and standard deviation values of the change of specific heat at glass transition temperature as function of amorphicity. For comparison, the glass transition temperature and the specific heat change were calculated for both (A) fictive and (B) half point temperatures.

Both correlation coefficients are good. This means that different synthetic mixtures give results that follow the same linear trend. There was no significant difference in the results at fictive and half point temperatures.

From the regression lines we obtain the numerical information for constants b, a, s_a and s_b using well-known equations [19]. LOD and LOQ values are calculated using the equations $X_L = 3s_a/b$ for LOD and $X_L = 10s_a/b$ for LOQ. LOD and LOQ values for the fictive temperature ($s_a = 7.341 \times 10^{-4}$, $b = 0.0070$) are 0.313% (amorphicity) and 1.04% and for the half point temperature ($s_a = 3.2444 \times 10^{-4}$, $b = 0.0068$) 0.107 and 0.358%, respectively.

In Table 7, the ΔC_p values are given as a function of the amorphous content. The experimental average and standard deviation values of ΔC_p are equal to values obtained from measurements of synthetic mixtures. For comparison there are two calculated values. The first values were calculated from the linear equation of synthetic mixtures. The second values were obtained by calculating the theoretical linear regression line between the average values given by 100% amorphous sample (precision studies) and zero and by calculating the corresponding values of different amorphous content from the equation. As can be seen in Table 7, there is no significant difference in the ΔC_p values of fictive and half point temperature. It can also be seen that experimental and calculated ΔC_p values are quite similar. Experimental values for low amorphous content are too large. This is result from the difficulty in preparing synthetic mixtures with a small amorphous content. Standard deviations in experimental values are small except at a high amorphous content.

3.4. Instrumental sensitivity and detection limit

No standard way exists for measuring the sensitivity of DSC peaks or glass transitions. The Dutch Society for Thermal Analysis (TAWN) has developed tests to measure the

Table 7
Comparison between experimental and calculated ΔC_p values

Amorphous content (%)	Experimental		Calculated ΔC_p ($J\,g^{-1}\,K^{-1}$)	
	ΔC_p ($J\,g^{-1}\,K^{-1}$)	S.D. ($J\,g^{-1}\,K^{-1}$)	Regression line of synthetic mixtures	Regression line of theoretical values
Fictive temperature				
100	0.630	0.146	0.704	0.727
75	0.465	0.039	0.529	0.545
50	0.344	0.054	0.353	0.364
25	0.218	0.020	0.178	0.182
20	0.138	0.020	0.143	0.145
15	0.101	0.008	0.107	0.109
10	0.073	0.001	0.072	0.073
7.5	0.052	0.008	0.055	0.055
5.2	0.034	0.004	0.039	0.038
1	0.008	0.001	0.009	0.007
0.5	0.009	0.003	0.006	0.004
0.1	0.005	0.002	0.003	0.001
Half point temperature				
100	0.708	0.095	0.684	0.706
75	0.503	0.016	0.513	0.530
50	0.344	0.043	0.343	0.353
25	0.211	0.017	0.172	0.177
20	0.158	0.021	0.138	0.141
15	0.098	0.011	0.104	0.106
10	0.072	0.002	0.070	0.071
7.5	0.053	0.019	0.053	0.053
5.2	0.036	0.007	0.037	0.037
1	0.008	0.000	0.008	0.007
0.5	0.009	0.003	0.005	0.004
0.1	0.005	0.002	0.002	0.001

The regression line of theoretical values is the theoretical linear regression between the average values given by 100% amorphous sample (precision studies) and zero (0% amorphous sample).

resolution and the sensitivity of DSC [20]. On the basis of their procedure we developed our own test to measure the sensitivity of our DSC. We took a small maltitol sample and melted it. The quenched glass was annealed and the glass transition was measured with different heating rates. The change of the heat flow of the glass transition was obtained as the difference of two straight lines, which represent the mean line before and after the glass transitions. Parallel to these lines two other lines were drawn such that all recorded data points were included between these two lines before or after the glass transition. The difference of these lines gave the sum of noise and heat flow drift.

The results of the sensitivity test are presented in Table 8. The heating rates used were 1, 10 and 100 °C min^{-1}. There were two maltitol samples, 0.900 and 0.646 mg, which average values are in Table 8. The system noise and heat flow drift were studied by performing measurements with an empty cup. The limit of detection was calculated by requiring the sensitivity to be ≥ 1. Also a percentage limit was calculated using a 10 mg sample.

The manufacturer had performed a baseline test of our new DSC and they reported the results together with their limits of acceptance (in parenthesis). The heat flow drift at 350 °C was 3.0 μW (<40 μW) and isothermal noise at 350 °C was 1.2 μW (<8.0 μW). These values are near our values at the heating rate 1 °C min^{-1}. With higher heating rates the heat flow drifts were reduced significantly and also noise was somewhat smaller. Simultaneously, the intensity of the glass transition signal increased. Therefore it is

Table 8
The results of sensitivity test. *a* is the average heat flow of two maltitol samples, *b* is the added values of noise and heat flow drift determined by using an empty cup and samples, and *a*/*b* is a measure of the sensitivity

Heating rate (°C min^{-1})	Empty cup	Sample			Detection limit	
	b (μW)	*a* (μW)	*b* (μW)	*a*/*b*	(g)	(%)
1	7.33	34	5.81	5.8	0.13	1.3
10	0.53	74	0.56	130	0.005	0.05
100	0.07	1070	0.14	7640	0.0001	0.001

Detection limit (%) is calculated for 10-mg sample.

possible get good sensitivity and also a low detection limit with high-speed heating.

Comparing the value of detection limit of heating rate 100 °C min^{-1} (Table 8) with experimental LOD value, it is possible to see that the experimental LOD is much higher than the instrumental limit of detection (Table 8). This means that the preparing of the synthetic amorphous maltitol samples was the weakest point in the determination of low amorphous levels in maltitol.

4. Conclusions

The preparation of synthetic test samples for determination of small amorphous content is difficult because amorphous maltitol absorbs moisture very readily. In addition, dried crystalline maltitol easily absorbs small amount of moisture if stored under normal room temperature and humidity. Although both crystalline and amorphous maltitol were stored over P_2O_5 before preparing synthetic mixtures, some moisture was present when measurements were started. This had a significant effect on the results. However, the results of experimental samples are satisfactory. The LOD and LOQ values are low and the instrumental sensitivity and LOD values are clearly better. Even better results could be obtained by optimising the experimental procedure. This study has established that hyper-DSC and the specific heat change at glass transition region constitute an efficient method for quantification of low amorphous content in maltitol.

Acknowledgements

Authors gratefully acknowledge the advice by H. Heikkilä and J. Nurmi and the financial support by Danisco Sweeteners. We also thank P. Robinson (Perkin-Elmer) for valuable advice for the determination of instrumental sensitivity.

References

[1] G.M. Venkatesh, M.E. Barnett, C. Owusu-Fordjour, M. Galop, Pharm. Res. 18 (2001) 98.
[2] G. Buckton, P. Darcy, Int. J. Pharm. 179 (1999) 141.
[3] P. Robinson, Abstract Book of ESTAC8, 2002, p. 101.
[4] Y. Roos, Carbohydr. Res. 238 (1993) 39.
[5] B. Wunderlich, Thermal Analysis, Academic Press Inc., San Diego, 1990, p. 101.
[6] Perkin-Elmer, Thermal Analysis Newsletter, Application Example PETAN-51.
[7] P. Claudy, M. Siniti, J. El Hajri, J. Therm. Anal. Calorim. 68 (2002) 251.
[8] Y. Roos, Phase Transitions in Foods, Academic Press Inc., San Diego, 1995, p. 110.
[9] B.C. Hancock, S.L. Shamblin, G. Zografi, Pharm. Res. 12 (1995) 799.
[10] A. Schouten, J.A. Kanters, J. Kroon, P. Looten, P. Duflot, M. Mathlouthi, Carbohydr. Res. 322 (1999) 298.
[11] Y.J. Park, J.M. Shin, W. Shin, I.-H. Suh, Bull. Korean Chem. Soc. 10 (1989) 352.
[12] S. Ohno, M. Hirao, Carbohydr. Res. 108 (1982) 163.
[13] N. Lebrun, J.C. van Miltenburg, J. Alloys Comp. 320 (2001) 320.
[14] O. Bustin, M. Descamps, J. Chem. Phys. 110 (1999) 10982.
[15] A. Raemy, T.F. Schweizer, J. Therm. Anal. 28 (1983) 95.
[16] M.J. Richardson, N.G. Savill, Polymer 16 (1975) 753.
[17] T.F.J. Pijpers, V.B.F. Mathot, B. Goderis, R.F. Scherrenberg, E.W. van der Vegte, Macromolecules 35 (2002) 3601.
[18] Microcal Origin, Version 6.1, Microcal Software, Inc., 1999.
[19] J.C. Miller, J.N. Miller, Statistics for Analytical Chemistry, third ed., Ellis Horwood, Chichester, UK, 1993, p. 104.
[20] P.J. van Ekeren, C.M. Holl, A.J. Witteveen, J. Therm. Anal. 49 (1997) 1105.